Journal of Engineering Science and Technology Review 16 (1) (2023) 52 - 60

Research Article

JOURNAL OF
Engineering Science and Technology Review

www.jestr.org

Ratio Analysis of Early Strength and Impermeable Anchoring Agent and its Anchoring Performance for Grotto

Zhehao Zhao[1], Jianhui Yang[1,*] and Liang Ye[1]

[1]*School of Civil Engineering and Architecture, Zhejiang University of Science and Technology, Hangzhou 310023, China*

Received 12 October 2022; Accepted 9 January 2023

Abstract

To solve the problem of water seepage in bolt holes and decrease of anchoring force during the hardening of traditional cement anchoring agents, a L16 (4^5) orthogonal test was carried out to test the fluidity, compressive strength and impermeability pressure indexes based on the water to binder ratio, expansive agent content, silica fume content, early strengthening agent content and superplasticizer content of the anchoring agent. Through the range analysis and analytic hierarchy method, a group of high early strength and good impermeability anchoring agent was preferred, and the bond strength of anchoring agent-rock interface was measured by the bolt pull-out test. Results show that the water to binder ratio is the most important factor affecting each index, and the weight of the remaining factors varies with the index. On the whole the influence of early strengthening agent and expansive agent is greater. The optimal ratio is 0.34 of water to binder ratio, 12% of expansive agent, 6.5% of silica fume, 3% of early strengthening agent and 0.44% of superplasticizer contents. By optimizing the mix ratio, the anchoring agent can have the early strength and impermeability, which can provide the reference for the grotto anchoring projects.

Keywords: Anchoring agent, Early strength and impermeability, Bond strength, Anchoring force

1. Introduction

As a valuable historical heritage of China, the grottoes record the development of the Chinese nation for five thousand years and contain rich cultural and artistic value. However, the humid climate in southern China is extremely unfavourable for grotto anchoring. Hence, to ensure the safety of grotto anchorage body, it is urgent to develop a cement anchoring agent with high early strength and good impermeability.

An underground grotto in southern Zhejiang, China is anchored with traditional cement. Such anchoring agent produces volume shrinkage during its hardening, so cracks are formed in the anchorage body, and its impermeability is so poor. Then the groundwater infiltrates into the grotto along the bolt hole, which adversely affects the rock mass of the grotto, and also reduces the anchoring force as a result. The studies have shown that the modified slurry with cement admixture can improve the early strength faster, and the anchorage body can achieve higher pull-out strength after curing with a lower engineering cost [1, 2].

High early cement strength is beneficial to improve anchorage quality and reduce the risk of early crack in grottoes. There are many reasons for the crack of cement anchorage agent. One of the most important ones is that the early strength of concrete is not enough and the curing is not enough. After the cement anchoring agent pouring, a certain amount of internal stress will produce due to the internal temperature and humidity changes in the structure. Taking account of the stress generated by the component itself and the external load, it is possible to exceed the tensile strength of the cement. Due to the influence of vibration and hydrostatic, the surface strength of cement slurry is lower than its internal strength, the surface structure of cement slurry is loose affected by external conditions. For the same grade of cement, the risk of crack is small if the early strength is high, or the curing time can be shortened, so improving the early strength of cement is conducive to improving the quality of cement anchorage agent.

Therefore, it is of great theoretical significance and practical value to study a cement anchoring agent with both high early strength and high impermeability. In addition, the rock varies greatly in different regions, the strength of red sandstone in southern Zhejiang is low, and the bond strength between anchoring agent and rock lacks relevant test data. Thus, relying on the red sandstone grottoes in southern Zhejiang, the early strength and impermeable anchoring agent and its bond property with red sandstone were studied, which can provide a foundation for the reinforcement of such grottoes.

2. State of the art

As a traditional and effective way of rock mass reinforcement, the anchorage technique has gained more and more applications in grotto protection. The early strength, impermeability and other indicators of the anchoring agent are the key contents of the research on grotto anchoring. Some scholars have carried out research on anchoring agents and grouts for general rock slope engineering, which provides reference for grotto anchoring engineering [3-5]. Liu et al. used fly ash, sodium silicate and other materials to improve the cohesion between the cement anchoring agent of the roadway and the rock mass, effectively controlled the deformation of the rock mass [6]. Cheng et al. carried out

*E-mail address: yjh0571@163.com
ISSN: 1791-2377
doi:10.25103/jestr.161.07

field pull-out tests of GFRP (Glass fiber reinforced polymer) and CFRP (Carbon fiber reinforced polymer) bolts, and they found that adding expansive agent to cement mortar could improve the anchoring performance [7]. Mollamahmutoglu et al. developed a slurry formed by a mixture of sodium silicate and boric acid, and they found that with the increase of sodium silicate content, the compressive strength of the slurry increased [8]. Salvatore et al. tested the setting rate, viscosity and shear strength of the grout after colloid nano silica was pressed into the grout by scanning electron microscopy and X-ray diffraction, proving that it had a good improvement effect, but the cost and performance needed to be considered comprehensively [9]. Xie et al. studied the influence of water seepage on the durability of CFRP bolts through pull-out tests, and they found that the water absorption of anchorage body was negatively correlated with the toughness of the bond medium at the anchoring interface [10]. Hu et al. added bentonite into cement mortar and found that the impermeability pressure of cement mortar mixed with 8% bentonite increased by 76.47%, because bentonite enhanced the refinement of microscopic pores [11]. Sanchez et al. pointed out the high-performance fiber-reinforced cement-based composite materials could be applied to the reinforcement process of concrete structures. This material possessed high compressive strength, low permeability, and the fiber could fully open at the crack, which significantly improved the load resistance and durability of concrete structures in the cracked state [12].

According to different contact media and contact surface, an anchorage body can be divided into three media: bolt, anchoring agent and surrounding rock, and two interfaces: bolt-anchoring agent and anchoring agent-surrounding rock. Among these elements, the strength characteristics of each medium are relatively stable while the bond place of each interface is very weak. After laying bolts for a long time, due to the shrinkage and deformation of anchoring agent, accompanied by humidity changes and other environmental factors, it is easy to lead to the loss of anchoring force. Scholars at home and abroad have carried out related research on the bond property of anchorage body interface. Wang et al. studied the mechanical performances of tension-torsion coupling anchor cable and the mechanical behavior of fully-grouted bolt in jointed rocks subjected to double shear tests [13, 14]. Chang et al. studied the pull-out performances of the grouted rockbolt systems with bond defects [15]. Du et al. summarized the factors influencing the bond strength of anchor and believed that the strength of anchorage agent and rock mass directly influenced the anchoring force [16]. To improve the bond strength of rock anchors, Liu et al. analyzed the influence of anchorage section length on bond strength and recommended the critical anchorage length value under specific geological conditions [17]. Han et al. conducted the analytical derivation of rib bearing angle of reinforcing bar subject to axial loading [18]. Mak & Lees studied the bond strength and confinement in reinforced concrete [19]. Abu Talha et al. conducted the laboratory evaluation of microsurfacing bond strength [20].

As the traditional cement anchorage produces volume shrinkage in the hardening process, the anchor solid produces cracks, and its impervious property is poor. Once the groundwater penetrates into the cave along the anchorage hole, the rock mass in the cave will be adversely affected, and the anchorage force will also be reduced. In this study, combining with a red sandstone grottoes project in southern Zhejiang region, the fluidity, 3 d and 7 d compressive strength, and 28 d impermeability pressure indexes of anchoring agents were determined by orthogonal test method with five factors and four levels. A group of target anchoring agents with high early strength and good impermeability was selected through the range analysis and analytic hierarchy process. The bond strength of the interface between anchoring agent and red sandstone was significantly improved by using this anchoring agent in low-strength red sandstone. The research results can provide the foundation for the grotto projects in southern Zhejiang, China.

The rest of this study is organized as follows. Section 3 introduces the test materials, orthogonal experiment design, test index and test methods. Section 4 analyzes the influencing factors of anchoring performance, the optimized mix ratio of anchoring agent, bond property between anchoring agent and surrounding rock, and finally, the conclusions are summarized in Section 5.

3. Methodology

3.1 Test materials

Materials selected for the test are listed as follows: P.I 42.5 reference cement was produced by Fushun Cement Ltd, its chemical composition was shown in Table 1. UEA expansive agent was produced in Nanchang County Huayu building Materials Factory. Silica fume was white powder, produced by Henan Yixiang New Material Ltd. Sodium sulfate early strengthening agent was produced by Yuncheng Tianming New Material Technology Ltd. FDN-C naphthalene water reducing agent was produced by Shandong Yousuo Chemical Technology Ltd, which was yellowish brown powder in appearance. Clean tap water was used as mixing water.

Table 1. Chemical composition of cement P.I 42.5

Name	SiO_2	Al_2O_3	Fe_2O_3	CaO	MgO	SO_3
Content (%)	20.60	4.57	3.29	63.27	2.59	2.11

3.2 Orthogonal experiment design

A type L_{16} (4^5) test scheme was designed according to the orthonormal test table, in which five factors were water to binder ratio, expansive agent content, silica fume content, early strengthening agent content and superplasticizer content. For convenience, the letter S represents the water-binder ratio, the letter P represents the expansion agent content, the letter G represents the silica fume content, the letter Z represents the early strength agent content, and the letter J represents the high efficiency water reducing agent content. The test factors and levels were listed in Table 2, and the orthogonal test scheme was shown in Table 3.

Table 2. Test factors and levels.

Level	S	P (%)	G (%)	Z (%)	J (%)
1	0.32	8	5.0	1	0.52
2	0.33	10	6.5	2	0.48
3	0.34	12	8.0	3	0.44
4	0.35	14	9.5	4	0.40

3.3 Test index and test methods

The fluidity test was conducted according to “Appendix A of Technical code for application of cementitious grout (GB/T 50448-2015) in China”.

The compressive strength at 3 d and 7 d of age was measured according to “Test method of cement mortar strength (GB/T 17671-2021) in China". According to "Standard for test method of performance on building mortar (JGJ/T 70-2009) in China" to complete the impermeability pressure test, a group of 6 specimens were cured in water for 28 d, then dried, sealed with neutral silicone weatherproof glue and dried for 24 h. After that, the specimens were put into the SJS-1.5S mortar impervious instrument, which could automatically control the pressure process. The seepage failure pressure was taken as the impermeability pressure when there was water on the upper surface of 3 specimens.

Table 3. Orthogonal test protocol.

No.	Factors				
	S	P (%)	G (%)	Z (%)	J (%)
1	0.32	8	5.0	1	0.52
2	0.32	10	6.5	2	0.48
3	0.32	12	8.0	3	0.44
4	0.32	14	9.5	4	0.40
5	0.33	8	6.5	3	0.40
6	0.33	10	5.0	4	0.44
7	0.33	12	9.5	1	0.48
8	0.33	14	8.0	2	0.52
9	0.34	8	8.0	4	0.48
10	0.34	10	9.5	3	0.52
11	0.34	12	5.0	2	0.40
12	0.34	14	6.5	1	0.44
13	0.35	8	9.5	2	0.44
14	0.35	10	8.0	1	0.40
15	0.35	12	6.5	4	0.52
16	0.35	14	5.0	3	0.48

The uniaxial compressive strength test was completed according to "Regulation for testing the physical and mechanical properties of rock-part 18: test for determining the uniaxial compressive strength of rock (DZ/T 0276.18-2015) in China". The diameter of the specimen was about 50 mm and the height-to-diameter ratio was 2.0. The tensile strength test of red sandstone was conducted according to "Regulation for testing the physical and mechanical properties of rock-part 21: test for determining the tensile strength of rock (DZ/T 0276.21-2015) in China". The diameter of the specimen was about 50 mm and the height-to-diameter ratio was 0.55.

The test scheme of interfacial bond strength between anchoring agent and red sandstone is designed according to "Technical code for engineering of ground anchorages and shotcrete support (GB 50086-2015) in China". To ensure that the interface between anchoring agent and rock being damaged during the pull-out test, a circular gasket was fixed with a nut at the anchorage end of the steel bar, as shown in Fig. 1.

Fig. 1. Steel bar specimen.

Six cube rock blocks with a side length of 200 mm were selected for the test piece. A 58 mm diameter bolt hole was drilled into each test piece, and a 16 mm diameter steel bar was inserted into the hole to simulate the bolt. The anchorage depth was 60 mm, and the steel bar was cured for 3 d and 7 d after grouting the anchoring agent. Finally, the early bond strength between anchoring agent and rock was calculated.

4. Results analysis and discussion

4.1 The mix of anchoring agent

The indexes measured by orthogonal test were analyzed. Firstly, range analysis method was used to determine the primary and secondary order of each factor, and then analytic hierarchy process was used to determine the influence weight of each factor on the indexes. The mix ratio of anchoring agent with high early strength and high impermeability was optimized, and the slurry was prepared according to this mix ratio.

4.1.1 Analysis of fluidity of anchoring agent

The test results of the fluidity, 3 d and 7 d compressive strength, and 28 d impermeability pressure of anchoring agent are shown in Table 4.

The range analysis data of the fluidity of anchoring agent are shown in Table 5, where j represents the five influencing factors (j=S, P, G, Z, J), i represents the four influencing levels of each factor (i=1, 2, 3, 4), K_{ij} represents the sum of indicators at level i under the influence of factor j, K_{ij}^* is the average value of K_{ij}, that is, $K_{ij}^* = \frac{1}{4} K_{ij}$. Range R_j is the difference between the maximum value and the minimum value of K_{ij}^* under the same influencing factor, that is, $R_j = \max\left\{K_{ij}^*\right\} - \min\left\{K_{ij}^*\right\}$.

It can be seen from Table 5, the range for the fluidity from large to small is $R_S > R_Z > R_P > R_J > R_G$, indicating that the order of each factor affecting the fluidity index is water to binder ratio > early strengthening agent content > expansive agent content > superplasticizer content > silica fume content.

According to the influence of various factors on the fluidity, the relationship diagram between the fluidity and the level of various factors is drawn, as shown in Fig. 2. With the increase of water to binder ratio, the fluidity increases, indicating that water to binder ratio is positively correlated with the fluidity. When the content of expansive agent increases, the fluidity decreases, and the minimum value appears when the content is 12 %. The reason for the decrease in fluidity is that C_4A_3S component of UEA expander consumes most of the water in the initial stage of hydration and generates ettringite crystals. When the content of silica fume increases, the fluidity first increases and then decreases. The reason for the increase of fluidity is the shape effect of the spherical vitreous particles for silica fume, which have a good lubrication during hydration and effectively reduce the resistance between the components. When the content of silica fume is more than 6.5 %, the fluidity decreases because of the filling effect and pozzolanic effect of silica fume. On the one hand, finer particles of silica fume fill the pores between the components of the slurry, making the whole gel system denser.

Table 4. Orthogonal test results.

No.	Fluidity (mm)	3 d compressive strength (MPa)	7 d compressive strength (MPa)	28 d impermeability pressure (MPa)
1	150	52.6	65.8	2.0
2	128	54.8	68.1	2.1
3	118	56.0	70.9	2.3
4	114	57.1	71.8	2.4
5	142	55.9	61.4	1.9
6	140	50.9	59.7	1.8
7	146	52.4	58.0	1.9
8	137	50.4	63.3	2.0

9	163	49.2	55.1	1.8
10	156	53.6	57.5	1.7
11	142	52.4	59.4	1.8
12	173	47.9	60.2	1.7
13	169	44.8	54.6	1.6
14	169	44.2	51.5	1.5
15	156	46.1	56.5	1.4
16	161	48.1	53.8	1.6

On the other hand, $Ca(OH)_2$ generated by cement hydration reacts with SiO_2 in the silica fume to continuously generate a large amount of CSH gel. The hydration process of cement is accelerated, and the fluidity is reduced macroscopically. When the content of early strengthening agent increases, the fluidity shows a decreasing trend, and decreases mostly when the content reaches 2%. The reason is that the sodium sulfate early strengthening agent participates in hydration faster than dihydrate gypsum in cement to generate calcium sulfoaluminate and the effect of early strength is achieved. The fluidity increases when the amount of superplasticizer increases on account of its ionization effect of the hydrophilic group to disperse the gel cement particles and release the water wrapped in the gel.

The water to binder ratio is the main factor affecting the fluidity, and the content of early strengthening agent, expansive agent and superplasticizer has a certain effect on the fluidity, the content of silica fume has the least effect on the fluidity. According to the influence of various factors on the fluidity, the relationship diagram between the fluidity and the level of various factors is drawn, as shown in Fig. 2.

As seen from Fig. 2, with the increase of water to binder ratio, the fluidity increases, indicating that water to binder ratio is positively correlated with the fluidity. When the content of expansive agent increases, the fluidity decreases, and the minimum value appears when the content is 12 %. The reason for the decrease in fluidity is that C_4A_3S component of UEA expander consumes most of the water in the initial stage of hydration and generates ettringite crystals. When the content of silica fume increases, the fluidity first increases and then decreases. The reason for the increase of fluidity is the shape effect of silica fume. The shape of the spherical vitreous particles can make it have a good lubrication during hydration and effectively reduce the resistance between the components. When the content of silica fume is more than 6.5 %, the fluidity decreases because of the filling effect and pozzolanic effect of silica fume. On the one hand, finer particles of silica fume fill the pores between the components of the slurry, making the whole gel system denser.

Table 5. Range analysis data of fluidity.

Index	Fluidity (mm)				
	S	P (%)	G (%)	Z (%)	J (%)
K_{1j}	510.00	624.00	593.00	638.00	599.00
K_{2j}	565.00	593.00	599.00	576.00	598.00
K_{3j}	634.00	562.00	587.00	577.00	600.00
K_{4j}	655.00	585.00	585.00	573.00	567.00
K^*_{1j}	127.50	156.00	148.25	159.50	149.75
K^*_{2j}	141.25	148.25	149.75	144.00	149.50
K^*_{3j}	158.50	140.50	146.75	144.25	150.00
K^*_{4j}	163.75	146.25	146.25	143.25	141.75
R_j	36.25	15.50	3.50	16.25	8.25

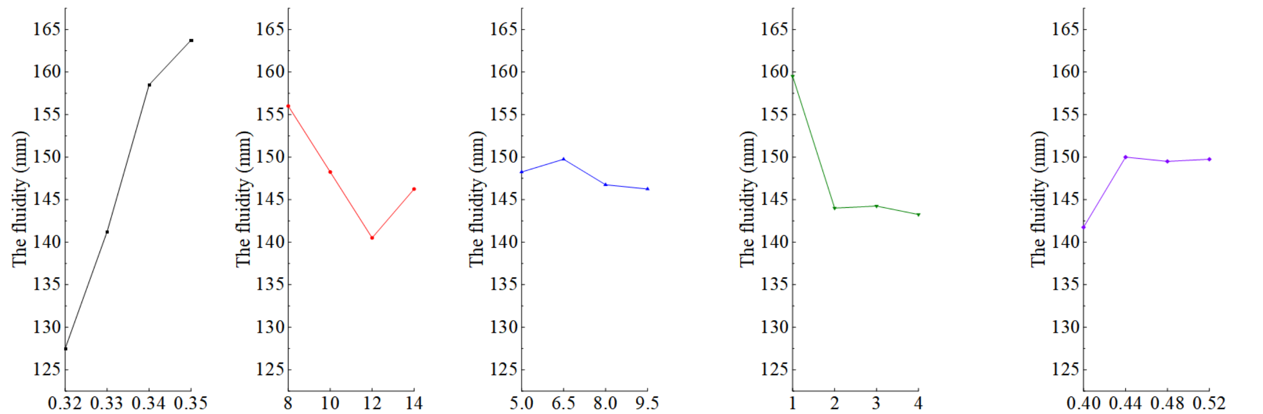

Fig. 2. Fluidity and factor level trends.

On the other hand, $Ca(OH)_2$ generated by cement hydration reacts with SiO_2 in the silica fume to continuously generate a large amount of CSH gel. The hydration process of cement is accelerated, and the fluidity is reduced macroscopically. When the content of early strengthening agent increases, the fluidity shows a decreasing trend, and decreases the most when the content reaches 2%. The reason is that the sodium sulfate early strengthening agent participates in hydration faster than dihydrate gypsum in cement to generate calcium sulfoaluminate and achieve the effect of early strength. When the amount of superplasticizer increases, the fluidity increases. The water reducing agent uses the ionization effect of the hydrophilic group to disperse the gel cement particles and release the water wrapped in the gel, so the superplasticizer can effectively increase the fluidity of the slurry.

4.1.2 Compressive strength analysis of anchoring agent

As shown in Tables 6 and 7, the 3 d compressive strength, the range from large to small is $R_S > R_Z > R_J > R_G > R_P$, indicating that the order of each factor affecting the 3 d compressive strength of anchoring agent is water to binder ratio > early strengthening agent content > superplasticizer content > silica fume content > expansive agent content. For the 7 d compressive strength, the range from large to small is $R_S > R_P > R_J > R_Z > R_G$, indicating that the order of the main factors affecting the 7 d compressive strength of anchoring agent is water to binder ratio > expansive agent content > superplasticizer content > early strengthening agent content > silica fume content. The water to binder ratio is the main factor affecting the 3 d and 7 d compressive strength. The content of expansive agent has the least effect on the 3 d compressive strength, and the content of silica fume has the least effect on the 7 d compressive strength. Fig. 3 shows the relationship diagram between the compressive strength and the level of various factors.

Table 6. Range analysis data of 3 d compressive strength.

Index	3 d compressive strength (MPa)				
	S	P (%)	G (%)	Z (%)	J (%)
K_{1j}	220.50	202.50	204.00	197.10	202.70
K_{2j}	209.60	203.50	204.70	202.40	204.50
K_{3j}	203.10	206.90	199.80	213.60	199.60
K_{4j}	183.20	203.50	207.90	203.30	209.60
K_{1j}^*	55.13	50.63	51.00	49.28	50.68
K_{2j}^*	52.40	50.88	51.18	50.60	51.13
K_{3j}^*	50.78	51.73	49.95	53.40	49.90
K_{4j}^*	45.80	50.88	51.98	50.83	52.40
R_j	9.33	1.10	2.02	4.12	2.50

As shown in Fig. 3, the compressive strength decreases with the increase of water to binder ratio, which conforms to the laws of mechanics. When the water to binder ratio is 0.35, the 3 d compressive strength reaches 45.80 MPa. "The water suction anchoring packet technical conditions (TB/T 2093-2002) in China" stipulates that the 3 d compressive strength of early strength anchoring agent should be greater than 30 MPa, and the 3 d compressive strength of high-strength anchoring agent should be greater than 40 MPa.

Table 7. Range analysis data of 7 d compressive strength.

Index	7 d compressive strength (MPa)				
	S	P (%)	G (%)	Z (%)	J (%)
K_{1j}	276.60	236.90	238.70	235.50	243.10
K_{2j}	242.40	236.80	246.20	245.40	235.00
K_{3j}	232.20	244.80	240.80	243.60	245.40
K_{4j}	216.40	249.10	241.90	243.10	244.10
K_{1j}^*	69.15	59.23	59.68	58.88	60.78
K_{2j}^*	60.60	59.20	61.55	61.35	58.75
K_{3j}^*	58.05	61.20	60.20	60.90	61.35
K_{4j}^*	54.10	62.28	60.48	60.78	61.03
R_j	15.05	3.08	1.88	2.47	2.60

With the increase of expansive agent content, the compressive strength shows an increasing trend, and the 7 d compressive strength increases more obviously. When the expansive agent content is 14%, the 7 d compressive strength increases by 11.41 MPa compared with the 3 d compressive strength, or about 22%. The 3 d compressive strength of the four groups with different expansive agent contents fluctuate around 51 MPa, and the curve is gentle, indicating that the effect of expansive agent on the 3 d compressive strength is small.

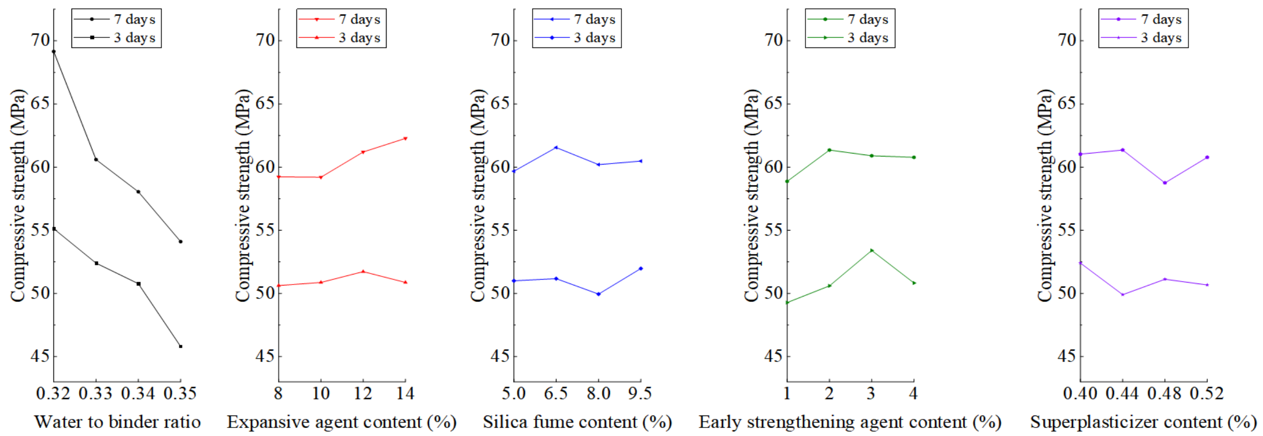

Fig. 3. Compressive strength and factor level trends.

The 3 d compressive strength of the four groups fluctuate at 51 MPa and the 7 d compressive strength fluctuate at 60 MPa, indicating that the influence of silica fume on the compressive strength is small. This indicates that in the process of cement hardening, expansive agent and early strengthening agent participate in hydration reaction before silica fume to produce those dense ettringites, and the bond process of ettringites is dense, so the pozzolash effect and filling effect of silica fume are not obvious, and the impact on compressive strength is small.

With the increase of the early strengthening agent content, the compressive strength first increases and then decreases, but it presents an increasing trend. It can be seen from Fig. 3, the 3 d compressive strength reaches the maximum value when the content of early strengthening agent is 3%, and the 7 d compressive strength reaches the maximum value when that is 2%. The 7 d compressive strength increases by 10.75 MPa, or about 21% compared with 3 d compressive strength when the content of early strengthening agent is 2%. The reasons for the first increase and then decrease of compressive strength are as follows: during the formation of ettringites, pores are filled first to make the system dense, leading to the increase of strength; but when the content of early strengthening agent continues to increase, more ettringites in the system extrude each other to form new cracks, then reducing the strength.

With the increase of superplasticizer content, the compressive strength shows a decreased trend on the whole. The reason is that the dispersion of superplasticizer makes the surface of cement particles with the same charge, which generates a repulsive force between the cement particles, so that the water in the flocculation structure is free from the inside to the surface, resulting in the loss of water. At the same time, in the process of water curing, the surface of the specimen is in direct contact with water, and the hydration is more adequate. However the internal components of the specimen are still in a state of water shortage compared with the surface, the strength decreases as a consequence of insufficient hydration [21]. When the superplasticizer content reaches 0.44-0.48% and 0.48-0.52 %, respectively, the 3 d compressive strength and 7 d compressive strength increase slightly. The reason may be that the ionization of the hydrophilic group of superplasticizer does not completely disperse the flocculation structure, so some particles agglomerate, and produce a small increase in strength. But the overall trend of compressive strength is still decreasing.

4.1.3 Impermeability pressure analysis of anchoring agent

As can be seen from Table 8, for 28 d impermeability pressure, the range from large to small is $R_S > R_P > R_G = R_J > R_Z$, indicating that the order of each factor affecting the 28 d impermeability pressure is water to binder ratio>expansive agent content > silica fume content = superplasticizer content > early strengthening agent content. The water to binder ratio is the main factor affecting the 28 d impermeability pressure, and the content of early strengthening agent has the least effect on 28 d impermeability pressure. The relationship between the impermeability pressure at 28 d and the levels of various factors can be seen in Fig. 4.

As shown in Fig. 4, with the increase of water to binder ratio, the impermeability pressure decreases, and the curve is steeper, indicating that the water to binder ratio has a great influence on 28 d impermeability pressure. When the water to binder ratio reaches 0.35, the impermeability pressure is about 1.5 MPa, which meets the requirements of "Technical code for waterproofing of underground works (GB 50108-2008) in China". As the content of superplasticizer increases, the impermeability pressure decreases on the whole. The reason lies in the effect of air-entraining of superplasticizer forms a considerable number of pores in the specimen, resulting in the decrease of impermeability pressure [22].

Table 8. Range analysis data of 28 days impermeability pressure

Index	28 d impermeability pressure (MPa)				
	S	P (%)	G (%)	Z (%)	J (%)
K_{1j}	8.80	7.30	7.20	7.10	7.10
K_{2j}	7.60	7.10	7.10	7.50	7.40
K_{3j}	7.00	7.40	7.60	7.50	7.40
K_{4j}	6.10	7.70	7.60	7.40	7.60
K_{1j}^*	2.20	1.83	1.80	1.78	1.78
K_{2j}^*	1.90	1.78	1.78	1.88	1.85
K_{3j}^*	1.75	1.85	1.90	1.88	1.85
K_{4j}^*	1.53	1.93	1.90	1.85	1.90
R_j	0.68	0.15	0.13	0.10	0.13

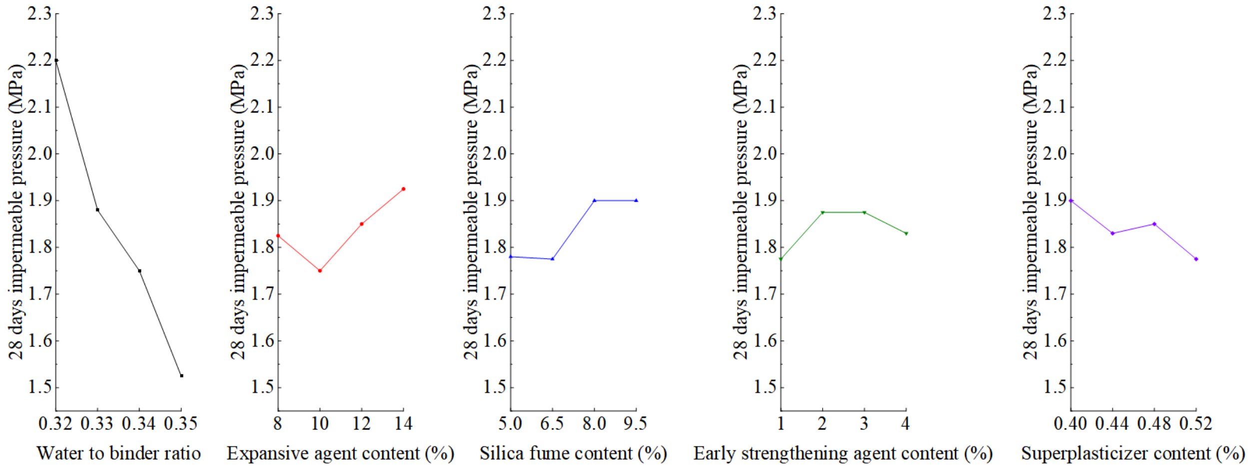

Fig. 4. 28 d impermeability pressure and factor level trends.

4.2 Weight analysis of influencing factors of anchoring performance

To determine these influence weights of water to binder ratio (S), expansive agent content (P), silica fume content (G), early strengthening agent content (Z) and superplasticizer content (J) on fluidity, 3 d compressive strength, 7 d compressive strength and 28 d impermeability pressure, the analytic hierarchy process is adopted to construct the hierarchical structure model. Then the decision matrix is constructed as well as the consistency of the matrix is tested. Fig. 5 shows the hierarchical structure model.

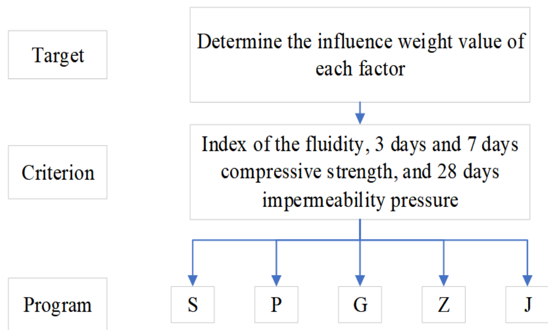

Fig. 5. Hierarchy model.

4.2.1 Analytic hierarchy process

According to the range of five factors in program on four indicators in criterion, combined with the decision matrix, the importance of each factor is scaled with levels 1-9. The scale of the decision matrix is shown in Table 9 [23].

The decision matrices A_1, A_2, A_3 and A_4 influencing the fluidity, the 3d compressive strength, the 7 d compressive strength and the 28 d impermeability pressure of anchoring agent are constructed below.

Table 9. Decision matrix scale definition.

Scale	Meaning
1	For two factors, the former is as important as the latter
3	For two factors, the former is slightly more important than the latter
5	For two factors, the former is obviously more important than the latter
7	For two factors, the former is strongly more important than the latter
9	For two factors, the former is extremely more important than

	the latter
2, 4, 6, 8	The median of the above adjacent scale
Reciprocal	For two factors, the importance scale of the latter compared to the former

$$A_1:\begin{pmatrix} 1 & 5 & 9 & 4 & 7 \\ \frac{1}{5} & 1 & 6 & \frac{1}{2} & 4 \\ \frac{1}{9} & \frac{1}{6} & 1 & \frac{1}{6} & \frac{1}{3} \\ \frac{1}{4} & 2 & 6 & 1 & 4 \\ \frac{1}{7} & \frac{1}{4} & 3 & \frac{1}{4} & 1 \end{pmatrix},\ A_2:\begin{pmatrix} 1 & 7 & 5 & 2 & 3 \\ \frac{1}{7} & 1 & \frac{1}{3} & \frac{1}{5} & \frac{1}{4} \\ \frac{1}{5} & 3 & 1 & \frac{1}{3} & \frac{1}{2} \\ \frac{1}{2} & 5 & 3 & 1 & 4 \\ \frac{1}{3} & 4 & 2 & \frac{1}{4} & 1 \end{pmatrix},$$

$$A_3:\begin{pmatrix} 1 & 6 & 9 & 8 & 7 \\ \frac{1}{6} & 1 & 4 & 3 & 2 \\ \frac{1}{9} & \frac{1}{4} & 1 & \frac{1}{2} & \frac{1}{3} \\ \frac{1}{8} & \frac{1}{3} & 2 & 1 & \frac{1}{2} \\ \frac{1}{7} & \frac{1}{2} & 3 & 2 & 1 \end{pmatrix},\ A_4:\begin{pmatrix} 1 & 4 & 5 & 6 & 5 \\ \frac{1}{4} & 1 & 2 & 3 & 2 \\ \frac{1}{5} & \frac{1}{2} & 1 & 2 & 1 \\ \frac{1}{6} & \frac{1}{3} & \frac{1}{2} & 1 & \frac{1}{2} \\ \frac{1}{5} & \frac{1}{2} & 1 & 2 & 1 \end{pmatrix}$$

4.2.2 Consistency test

The results of analytic hierarchy process of the influencing factors on fluidity, 3 d, 7 d compressive strength and 28 d impermeability pressure of anchoring agent are shown in Table 10.

Table 10. Analytic hierarchy results.

Test index	Analytic hierarchy index	Factors				
		S	P (%)	G (%)	Z (%)	J (%)
Fluidity	Eigenvector	2.646	0.806	0.174	1.038	0.337
	Weight (%)	52.911	16.112	3.472	20.765	6.740
	Largest eigenvalue	5.296				
	Consistency ratio	0.066				
The 3 d compressive strength	Eigenvector	2.122	0.226	0.475	1.466	0.710
	Weight (%)	42.444	4.530	9.508	29.319	14.200
	Largest eigenvalue	5.200				
	Consistency ratio	0.045				
The 7 d compressive strength	Eigenvector	3.061	0.834	0.221	0.342	0.542
	Weight (%)	61.216	16.672	4.414	6.850	10.848
	Largest eigenvalue	5.154				
	Consistency ratio	0.034				
The 28 d impermeability pressure	Eigenvector	2.663	0.931	0.542	0.321	0.542
	Weight (%)	53.265	18.617	10.848	6.421	10.848
	Largest eigenvalue	5.065				
	Consistency ratio	0.015				

After the consistency test, the consistency ratio of each test index is listed in Table 10. The consistency ratio of each index in the table is less than 0.1, indicating that the decision matrix meets the consistency test. In addition, the weight ranking of each factor obtained by analytic hierarchy process is consistent with the result of range analysis, which indicates that the analytic hierarchy process is reasonable.

The results of analytic hierarchy process shows that among the five influencing factors, the water to binder ratio has the greatest influence on each index. Among those indexes, the influence weight of water to binder ratio on fluidity, 7 d compressive strength and 28 d impermeability pressure is more than 50%, and the influence weight on 3 d compressive strength is more than 40%. Therefore, it is vital to strictly control the water to binder ratio in practical engineering.

In terms of early strength indexes, it is found that the main factors are water to binder ratio, early strengthening agent content and superplasticizer content, with weights of 42.44%, 29.32% and 14.20%, respectively. The main factors affecting the 7 d compressive strength are water to binder ratio, expansive agent content and superplasticizer content, with weights of 61.22%, 16.67% and 10.85%, respectively. It is not difficult to find that in addition to the water to binder ratio, the content of early strengthening agent, expansive agent and superplasticizer plays a certain role in improving the early strength of anchoring agent, thus it is needed to pay attention to the contents and strictly controll them in engineering.

In terms of impermeability pressure index, apart from water to binder ratio, expansive agent content has the greatest influence weight of 18.62%. Early strengthening agent has the least effect on 28 d impermeability pressure. Therefore, the content of expansive agent should be strictly controlled in engineering practice in order to the better impermeability of anchoring agent.

4.3 The optimized mix ratio of anchoring agent

Through the above analysis, the optimal mix ratio scheme with a single index is obtained, that is, the optimal content determined by the indexes of fluidity, 3 d compressive strength, 7 d compressive strength, 28 d impermeability pressure are $S_4P_1G_2Z_1J_3$, $S_1P_3G_4Z_3J_4$, $S_1P_4G_2Z_2J_3$, $S_1P_4G_3Z_3J_4$, respectively.

If a single index is used as the basis to determine the optimal content, the obtained optimal content varies with the index and is not representative. Therefore, the optimal content should be determined by taking into account the fluidity, early strength, impermeability pressure indexes, and actual engineering requirements. By observing the compressive strength of 3 d & 7 d and impermeability pressure of 28 d, it is concluded that the content of silica fume is 6.5% and the content of superplasticizer is 0.44 %. To facilitate the construction, the fluidity index should be controlled within the range of 150-210 mm, so the water to binder ratio of 0.34 is selected [24]. Combined with the 3 d compressive strength index, it is found that the strength decreases when the content of expansive agent increases to 14%, and a similar rule is found when the content of early strengthening agent is greater than 3%. Therefore, the content of expansive agent 12% and early strengthening agent 3% are selected. After comprehensive evaluation, the optimal content of anchoring agent is $S_3P_3G_2Z_3J_3$.

After the mix ratio is obtained, the tests are carried out according to the mix ratio, and the measured fluidity of the anchoring agent is 155 mm, the 3 d compressive strength is

52.3 MPa, the 7 d compressive strength is 58.7 MPa, and the 28 d impermeability pressure is 1.7 MPa. All indexes meet the requirements of the specification

4.4 Bond property analysis between anchoring agent and surrounding rock

4.4.1 Tensile and compressive strength tests of red sandstone

Two compressive specimens and four splitting specimens are prepared, and the failure forms of the specimens are shown in Fig. 6.

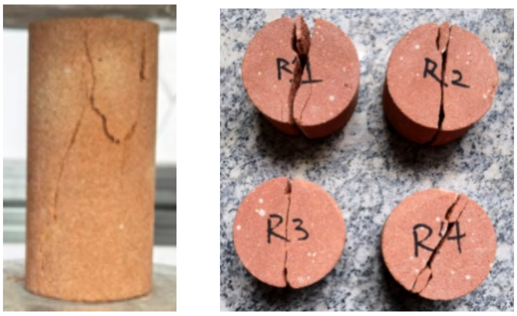

(a) Compressive specimen (b) Splitting specimen

Fig. 2. Sample of red sandstone.

The uniaxial compressive strength and tensile strength of the specimen are calculated, and the results are listed in Table 11.

Table 11. Tensile and the uniaxial compressive strength of red sandstone.

Name	No.	Size		Strength (MPa)	Average strength (MPa)
		Diameter (mm)	Height (mm)		
Compressive specimen	Y_1	49.18	100.51	24.97	25.01
	Y_2	49.30	99.62	25.04	
Tensile specimen	R_1	49.21	27.27	1.70	1.70
	R_2	49.29	27.41	1.60	
	R_3	49.24	27.75	1.80	

As shown in Table 11, the average compressive strength is about 25.01 MPa and the average tensile strength is about 1.7 MPa. Combined with the classification standard of uniaxial compressive strength of rock blocks, the uniaxial compressive strength of this red sandstone is low. As can be seen from in Fig. 6, fracture inclined plane appears on the surface of the specimen, resulting in single inclined shear failure. Numerically, the ratio of tensile strength to uniaxial compressive strength is about 0.07.

4.4.2 Bond strength test between anchoring agent and red sandstone

Due to the small anchorage length, the shear stress at any point of the anchoring interface can be approximately regarded as uniform distribution [25]. Therefore, the bond strength of the interface between anchoring agent and surrounding rock can be calculated according to Eq. (1):

$$\tau = \frac{P}{\pi d l} \tag{1}$$

where, τ is the bond strength (MPa), P is the ultimate pullout capacity (kN), d is the diameter of the bolt hole (mm), l is the anchorage length (mm).

The ultimate pullout capacity test results are listed in Table 12, and the anchor after the pull-out test is shown in Fig. 7. As can be seen from Table 12, the average values of the bond strength between the anchoring agent and surrounding rock at 3 d and 7 d are 2.60 MPa and 2.89 MPa, respectively. “Technical code for engineering of ground anchorages and shotcrete support (GB 50086-2015) in China” stipulates that the standard limit bond strength of soft rock should meet 0.6-1.2 MPa. As the 3 d bond strength measured by tests is much greater than the above value, meeting the requirements of the specification. As can be seen from Fig. 7, a layer of red sandstone is attached to the surface of the anchoring agent when the steel bar is pulled out, indicating that the interface between the anchoring agent and surrounding rock is damaged during the pull-out test, and the test results are in line with expectations.

Table 12. Bolt ultimate pull-out capacity and bond strength

Name	Size		Ages (d)	Ultimate pullout capacity (kN)	Bond strength (MPa)
	Diameter of bolt hole (mm)	Anchorage length (mm)			
R_1	58	60	3	28.52	2.61
R_2	58	60	3	27.47	2.51
R_3	58	60	3	29.31	2.68
Average value	-	-	-	28.43	2.60
R_4	58	60	7	31.35	2.87
R_5	58	60	7	30.61	2.80
R_6	58	60	7	32.84	3.00
Average value	-	-	-	31.60	2.89

Fig. 3. Bolt after the pull-out test.

5. Conclusions

To solve the problem of water seepage in bolt holes and decrease of anchoring force during the hardening of traditional cement anchoring agents, the influence trend and influence weight of each factor and level on the fluidity were analyzed, the compressive strength and impermeability pressure by means of range and analytic hierarchy process were studied combining with the rock block compressive strength and tensile strength test and the bolt pull-out test, the main conclusions are obtained as follows:

Among the five factors affecting the fluidity, 3 d and 7 d compressive strength, 28 d impermeability pressure indexes, the water to binder ratio has the greatest influence among all indexes. Except 3 d compressive strength, the influence weight of water to binder ratio on other indexes is more than 50%. Furthermore, the influence of the early strengthening agent content on fluidity and 3 d compressive strength is second only to the water to binder ratio. In terms of 7 d compressive strength and 28 d impermeability pressure, the influence of expansive agent content is second only to the water to binder ratio. Therefore, the water to binder ratio, the early strengthening agent content and the expansive agent content should be strictly controlled in practical engineering.

Comprehensively considering the fluidity, early strength and 28 d impermeability pressure index , combined with the actual project, the optimal mix ratio of anchoring agent is determined: water to binder ratio of 0.34, expansive agent content of 12%, silica fume content of 6.5%, early strengthening agent content of 3%, superplasticizer content of 0.44%. All indexes of the mixture ratio meet the requirements of the specification, and the anchoring agent has the performance of early strength and impermeability.

The uniaxial compressive strength of red sandstone is about 25.01 MPa, which is relatively low. The failure mode shows that shear failure occurs under uniaxial pressure. The tensile strength of red sandstone is about 1.7 MPa, and the ratio of tensile strength to compressive strength is about 0.07. The pull-out test exhibits that the optimal anchoring agent can effectively improve the bond strength of the interface between anchoring agent and red sandstone, reaching 2.60 MPa in 3 d and 2.89 MPa in 7 d, which meets the specifications and engineering requirements.

Due to the different rock strength and groundwater distribution of grottoes in different areas, the anchoring effect of early strength and impermeable anchoring agents on rock mass will be different, and the anchoring force that can be achieved at certain ages will also be different. In the future, anchoring agents with higher strength and better impermeability will be further studied so as to provide a foundation for more rock anchoring projects.

Acknowledgements
This work was financially supported by the National Natural Science Foundation of China (52008372).

References

1.Komurlu, E., “An Investigation of using thermoset polymer type liquid additives to improve cement grout performances in rock bolting applications”. *International Journal of Geosynthetics and Ground Engineering*, 6(4), 2020, pp. 1-13.

2.Krivenko, P. V., Petropavlovskyi, O. M., Rudenko,I. I., Konstantynovskyi, O. P., Kovalchuk, A. V., “Complex multifunctional additive for anchoring grout based on alkali-activated portland cement”. *IOP Conf. Series: Materials Science and Engineering*, 907, 2020, pp. 012055.

3.Augustine, R. L., Tanielyan, S. K., Mahata, N., Gao, Y., Zsigmond, A., Yang, H., “Anchored homogeneous catalysts: the role of the heteropoly acid anchoring agent”. *Applied Catalysis A: General*, 256(1-2), 2003, pp. 69-76.

4.Kan, J. G., Sun, Y. T., Wang, Y. F., Yang, S., Wang, P., “Experimental investigation on stirring rate affecting bubble structure of resin anchor agent and anchoring strength”. *Advances in Materials Science and Engineering*, 2020, 2020, pp. 8839390.

5.Duan, Z. Q., Qu, Z. Y., Hu, F. L., Yang, Y. X., Chen, G. R., Xu, H., “Quantification of surface-anchored RAFT chain transfer agent on silica particles”. *Applied Surface Science*, 300, 2014, pp. 104-110.

6.Liu, F., Zou, Q., Liu, Y., “Effect of optimizing proportioning parameters of anchor material on anchoring system”. *Safety in Coal Mines,* 53(4), 2022, pp. 224-229.

7.Cheng, Y. M., Au, S. K., Yeung, A. T., “Laboratory and field evaluation of several types of soil nails for different geological conditions”. *Canadian Geotechnical Journal*, 53(4), 2016, pp. 634-645.

8.Mollamahmutoglu, M., Avci, E., Toma, S. K., Kose, D. A., “Performance of novel chemical grout in treating sands”. *Journal of Materials in Civil Engineering*, 29(10), 2017, pp. 152-164.

9. Salvatore, E., Modoni, G., Mascolo, M. C., Grassi, D., Spagnoli, G., “Experimental evidence of the effectiveness and applicability of colloidal nanosilica grouting for liquefaction mitigation”. *Journal of Geotechnical and Geoenvironmental Engineering*, 146(10), 2020, pp. 100-108.

10.Xie, G. H., Yan, P., Sun, Y., Feng, Q. H., Gedi, A. A., “Fatigue performance of anchorage for CFRP tendons affected by water infiltration”. *Construction and Building Materials*, 269, 2021, pp. 121359.

11. Hu, Y., Diao, L., Lai, Z. Y., He, Y. J., Yan, T., He, X., Wu, J., Lu, Z. Y., Lv, S. Z., “Effects of bentonite on pore structure and permeability of cement mortar”. *Construction and Building Materials*, 224, 2019, pp. 276-283.

12.Sanchez, M., Faria, P., Ferrara, L., Horszczaruk, E., Jonkers, H. M., Kwiecien, A., Mosa, J., Peled, A., Pereira, A. S., Snoeck, D., Stefanidou, M., Stryszewska, T., Zajac, B., “External treatments for the preventive repair of existing constructions: A review”. *Construction and Building Materials*, 193, 2018, pp. 435-452.

13. Wang, S. R., Xiao, H. G., Zou, Z. S., Cao, C., Wang, Y. H., Wang, Z. L., “Mechanical performances of transverse rib bar during pull-out test”. *International Journal of Applied Mechanics*, 11(5), 2019, pp. 1950048.

14.Wang, S. G., Xiao, H. G., Hagan, P., Zou, Z. S., “Mechanical behavior of fully-grouted bolt in jointed rocks subjected to double shear tests”. *DYNA*, 92(3), 2017, pp. 314-320..

15. Chang, X., Li, Z. H., Wang, S. Y., Wang, S. R., Fu, L., Tang, C. A., “Pullout performances of grouted rockbolt systems with bond defects”. *Rock Mechanics and Rock Engineering*, 51, 2018, PP. 861-871.

16. Du, F. Z., Gao, X. F., Gao, F. Q., “Research status-quo of anchored force test for anchored bolt”. *Coal mining Technology*, 14(3), 2009, pp. 1-4.

17. Liu H., Wang, X. D., Sheng, G. Q., “Experimental study of adhesion strength between rock anchor grout and rock for a slope stability project”. *Soil Engineering and Foundation*, 35(6), 2021, pp. 777-780.

18.Han, J., Wang, S. R., Chen, Y., Cao, C., “Analytical derivation of rib bearing angle of reinforcing bar subject to axial loading”. *Magazine of Concrete Research*, 71(4), 2019, pp. 175-183.

19.Mak, M. W. T., Lees, J. M., “Bond strength and confinement in reinforced concrete”. *Construction and Building Materials*, 355, 2022, pp. 129012.

20. Abu Talha, S., Al-Hosainat, A., Nazzal, M. D., Kim, S. S., Abbas, A., Mohammad, L. N., Nassar, S., “Laboratory evaluation of microsurfacing bond strength”. *Journal of Materials in Civil Engineering*, 34(2), 2022, pp. 04021444.

21.Kilinckale, F. M., Dogan, G. G., “Performance of concretes produced with superplasticizer”. *Journal of Applied Polymer Science*, 103(5), 2007,. pp. 3214-3219.

22.Yin, H. J., He, Y. F., Fu, C. Q., “Pressure transient analysis of heterogenous reservoirs with impermeability barrier using perturba-tion boundary element method”. Journal of Hydrodynamics, 17(1), 2005, pp. 102-109.

23.Lončarić, N., Keček, D., Kraljić, M., “Matrices in computer graphics”. Technical Journal, 12(2), 2018, pp. 120-123.

24.Wang, S. R., Shi, K. P., Chen, Y. B., Zhang, J. Y., Li, C. L., “Analysis on strength characteristics and energy dissipation of improved-subgrade soil of high-speed railway above mined-out areas”. *Tehnički vjesnik-Technical Gazette*, 30(1), 2023, pp. 256-264.

25.Wang, S. R., Wang, Y. H., Gong, J., Wang, Z. L., Huang, Q. X., Kong, F. L., “Failure mechanism and constitutive relation for an anchorage segment of an anchor cable under pull-out loading”. *Acta Mechanica*, 231(8), 2020, pp. 3305-3317.